Relativistic calculations of ground and excited states of LiYb molecule for ultracold photoassociation spectroscopy studies

Geetha Gopakumar,[1,a)] Minori Abe,[1] Bhanu Pratap Das,[2] Masahiko Hada,[1] and Kimihiko Hirao[3]
[1]*Department of Chemistry, Tokyo Metropolitan University, 1-1 Minami-Osawa, Hachioji-shi, Tokyo 192-0397, Japan*
[2]*Non Accelerator Particle Physics Group, Indian Institute of Astrophysics, Koramangala, Banglore 560 034, India*
[3]*Next-Generation Molecular Theory Unit, RIKEN, 2-1, Hirosawa, Wako, Saitama 351-0198, Japan*

(Received 11 February 2010; accepted 15 July 2010; published online 29 September 2010)

We report a series of quantum-chemical calculations for the ground and some of the low-lying excited states of an isolated LiYb molecule by the spin-orbit multistate complete active space second-order perturbation theory (SO-MS-CASPT2). Potential energy curves, spectroscopic constants, and transition dipole moments (TDMs) at both spin-free and spin-orbit levels are obtained. Large spin-orbit effects especially in the TDMs of the molecular states dissociating to $Yb(^3P_{0,1,2})$ excited states are found. To ensure the reliability of our calculations, we test five types of incremental basis sets and study their effect on the equilibrium distance and dissociation energy of the ground state. We also compare CASPT2 and CCSD(T) results for the ground state spectroscopic constants at the spin-free relativistic level. The discrepancies between the CASPT2 and CCSD(T) results are only 0.01 Å in equilibrium bond distance (R_e) and 200 cm^{-1} in dissociation energy (D_e). Our CASPT2 calculation in the supermolecular state (R=100 a.u.) with the largest basis set reproduces experimental atomic excitation energies within 3% error. Transition dipole moments of the super molecular state (R=100 a.u.) dissociating to $Li(^2P)$ excited states are quite close to experimental atomic TDMs as compared to the $Yb(^3P)$ and $Yb(^1P)$ excited states. The information obtained from this work would be useful for ultracold photoassociation experiments on LiYb. © *2010 American Institute of Physics*. [doi:10.1063/1.3475568]

I. INTRODUCTION

Ultracold atomic quantum gases are very dilute systems (typically below 10^{15} cm^{-3}). Nevertheless, interatomic interactions determine many of the phenomena observed in Bose–Einstein condensation,[1–3] quantum degenerate Fermi gases,[4] and other correlated systems. Usually, only the short-range isotropic contact interaction plays a role in quantum degenerate gases. However, recent developments in the manipulation of cold atoms and molecules are paving the way for the analysis of polar gases in which anisotropic long-range dipole-dipole interatomic interactions[5] are important. Indeed, experiments[6] on cooling and trapping of polar molecules as well as on photoassociation[7] and on Feshbach resonances[8,9] in binary mixtures of ultracold atoms have opened up exciting possibilities. Many applications using polar molecules, which have large anisotropic interactions, have also been theoretically proposed.[10] To study such long-range interactions, an experiment is being planned for the production of ultracold polar molecules from ultracold lithium (Li) and ytterbium (Yb) atoms.[11] Among the species cooled so far to the ultracold regime, LiYb was chosen due to its large mass ratio ($M_{Yb}/M_{Li} \sim 29$) among the constituent species. The most important advantage of LiYb is the existence of a spin degree of freedom in the ground molecular state, which enables it to be implemented as quantum simulator of lattice-spin models.[12] The experiment[13] on the simultaneous magneto-optical trapping of Li and Yb atoms for the production of ultracold LiYb molecule and collisional experiments are underway.

Photoassociation (PA) spectroscopy in ultracold atoms has become one of the most powerful tools for high-resolution molecular spectroscopy. In PA spectroscopy, a pair of ultracold ground state atoms absorbs a photon and a molecule is created in a rovibrational level of an excited electronic state. Another photon transfers this rovibrational level of the excited state to the electronic ground state with v=0, through stimulated emission. The photoassociation laser for this experiment is chosen in such a way that its frequency is detuned to the S-P transition. This transition typically occurs at large interatomic distances and the PA spectrum provides crucial information about long-range interactions in molecules and the collisional properties of atoms, which are difficult to obtain by other conventional spectroscopic experiments.

Preliminary theoretical studies based on quantum chemistry are very important to support the ongoing PA experiments. First and foremost contribution of the theory is to provide accurate and detailed potential energy curves (PECs) and transition dipole moments (TDMs) for the ground and low-lying excited states of LiYb at electronic levels. Based on the reliable PECs and TDMs, we could consider rovibra-

a)Electronic mail: geetha@tmu.ac.jp.

tional or scattering wave functions further, which are more concrete and important to decide the type of laser for PA transition in experiments. Determination of the permanent dipole moment (PDM) of the ground (v=0) state is also an important requisite as an indicator of the strength of the dipolar interactions in these systems.

This paper is devoted to calculating reliable PECs and TDMs of the ground and low-lying excited states of LiYb. Note here that the electronic ground-state configuration of $Li(^2S_{1/2})$ is $(1s)^2(2s)^1(2p)^0$ and that of $Yb(^1S_0)$ is [Xe-core] $(4f)^{14}(6s)^2(6p)^0$. We have included all the electronic states which dissociate to $Li(^2S_{1/2})+Yb(^1S_0)$, $Li(^2P_{1/2,3/2})+Yb(^1S_0)$, $Li(^2S_{1/2})+Yb(^3P_{0,1,2})$, and $Li(^2S_{1/2})+Yb(^1P_1)$ because they are the candidate states of S-P transition in PA experiments in LiYb. The LiYb molecular bond in the ground state is very weak because of the closed shell structure of Yb 6*s* orbital and hence, we need to use an appropriate method for carrying out calculations on this molecule. There is experimental data on LiYb system using mass spectrometry,[14] but it only provides ground state spectroscopic constants and further work including information on the excited states are necessary. The spin-orbit (SO) effect, which is relativistic in origin, is also expected to be important especially for higher excited states, since Yb is a heavy element (atomic number 70). Hence, we adopted the complete active space second-order perturbation theory (CASPT2) method considering both spin-free (SF) and spin-orbit relativistic effects using MOLCAS software.[15] This technique, SO-CASPT2, is nowadays widely applied and gives satisfactory results for small molecules with heavy elements.[16]

To confirm the reliability of the CASPT2 method for LiYb, we first calculated the ground state spectroscopic constants by the CCSD(T) method and compared with the CASPT2 results within the spin-free relativistic framework. We also investigated the basis set dependence of the spectroscopic constants of the ground state, using various sizes of relativistic correlation-consistent atomic natural orbital (RCC-ANO) basis sets.[17] As we discuss in Sec. III A, the largest RCC-ANO basis set is found to be important to describe the shallow potential curve of the ground state of LiYb. The difference between the CASPT2 and CCSD(T) results in the spectroscopic constants is acceptably small with this largest basis set. Based on this result, we have calculated multielectronic states with the SO-CASPT2 method and proposed theoretical spectroscopic constants. Supermolecular calculations (R_{LiYb}=100 a.u.) by the SO-CASPT2 method reproduce experimental atomic excitation energies[18] of Yb and Li within 3%. We also computed and analyzed TDMs between the ground and the excited states as functions of nuclear distance at spin-free and spin-orbit level. PDM values of the ground state at the equilibrium nuclear distance both at spin-free and spin-orbit levels are also presented.

TABLE I. Incremental basis set used in the systematic study of the ground state LiYb molecule.

Name of the basis in the text	Li RCC-ANO $12s11p8d7f4g2h$	Yb RCC-ANO $25s22p15d11f4g2h$
Basis 1	$5s4p2d1f$	$8s7p4d3f2g1h$
Basis 2	$5s4p2d1f$	$9s8p5d4f3g2h$
Basis 3	$5s4p2d1f$	$10s9p6d5f4g2h$
Basis 4	$8s7p4d2f$	$11s10p7d6f4g2h$
Basis 5	$8s7p4d2f$	$12s11p8d7f4g2h$

II. CALCULATION DETAILS

For all the calculations throughout this study, we employed MOLCAS 7.2 version code.[15] We used C_{2v} point group for symmetry considerations. Scalar relativistic effects are taken through the third order Douglas–Kroll–Hess (DKH)[19,20] transformation of the relativistic Hamiltonian.

We have calculated the equilibrium bond distance (R_e) and dissociation energy (D_e) of the LiYb ground state using open-shell Møller–Plesset second order perturbation theory (MP2),[21] coupled cluster singles and doubles with partial triples (CCSD(T)), and CASPT2 methods to investigate how electron correlation is important for this system. In both open-shell MP2 and CCSD(T) calculations, all the core electrons below Yb (4*d*) are frozen and hence the excitations are considered from Li 1*s* and 2*s* and Yb 5*s*, 5*p*, 4*f*, and 6*s* orbitals. For CASSCF and CASPT2, the CAS space is considered as all possible excitations of three electrons from/to eight space orbitals, which mainly belong to Li 2*s* and 2*p* and Yb 6*s* and 6*p* atomic orbitals. Frozen core orbital space in CASPT2 is same as the space of open-shell MP2 and CCSD(T).

The all electron relativistic correlation consistent basis set (RCC-ANO) is used for the calculations. The Yb and Li basis sets are contracted from the primitives Yb($25s22p15d11f4g2h$) and Li($14s9p4d3f1g$). Basis set dependence in conjugation with basis set convergence are studied by employing five different basis sets as tabulated in Table I. We start with a triple zeta quality (Yb:$8s7p4d3f2g1h$ and Li:$5s4p2d1f$) and increment them leading to the largest basis available in the basis set library. Throughout this paper, we will be pointing to the basis sets in numbers in ascending order. For Yb atom, all the symmetries (*s*, *p*, *d*, and *f*) except *g* and *h* are incremented step by step from basis 1 to 5. For Li atom, we have used two different kinds of basis: $5s4p2d1f$ (basis 1 to 3) and $8s7p4d2f$ (basis 4 to 5). The largest basis set in total has 255 basis functions. We also check basis set super position error (BSSE) using the counterpoise correction (CPC) method. For these calculations, spin-orbit effects are neglected. To obtain R_e and D_e, the ground state molecular potential curve is fitted with a third order polynomial using five points (0.05 a.u. spacing) around the equilibrium distance. Calculations of supermolecular system with 100 a.u. of Li–Yb bond distance are compared with atomic limit ($Li_{atom}+Yb_{atom}$) calculations as a check of the size consistency of the correlation methods employed.

From the above methodological study on the ground state LiYb, we selected the largest contraction type of RCC-ANO as the most suitable basis set in this system. We em-

ployed CASSCF/CASPT2 method as a suitable electron correlation method to describe multielectronic states of LiYb system. We obtained state averaged (SA) CASSCF wave functions with the following root numbers in the irreducible representations (irreps) of C_{2v} with doublet and quartet spin states: $^2A_1:3$, $^2B_1:2$, $^2B_2:2$, $^2A_2:0$, $^4A_1:1$, $^4B_1:1$, $^4B_2:1$, and $^4A_2:0$. The numbers of roots in each of the irreps were decided by considering only the states which dissociate to $Li(^2S_{1/2})+Yb(^1S_0)$, $Li(^2P_{1/2,3/2})+Yb(^1S_0)$, and $Li(^2S_{1/2})+Yb(^3P_{0,1,2})$. Within each irrep, we used equivalent weight for averaging. Energy levels of the $4\ ^2\Sigma$ and the $3\ ^2\Pi$ state, dissociating to $Yb(^1P_1)$, are calculated although these states and are not included in the state-averaging process. Multistate (MS) CASPT2 method is employed with the above SA-CASSCF states with the following root numbers in the irreps: $^2A_1:4$, $^2B_1:3$, $^2B_2:3$, $^2A_2:0$, $^4A_1:1$, $^4B_1:1$, $^4B_2:1$, and $^4A_2:0$. The correlation space for the CASSCF/CASPT2 calculation is same as the previous study of the ground state. The standard IPEA-H0 Hamiltonian[22] is used in CASPT2. We also used imaginary shift[23] (0.1 hartree) to remove the spikes from the CASPT2 potential energy curves. First-order spin-orbit effects are perturbatively considered using the DKH transformation with the atomic mean field integrals.[24] All the states obtained in the CASSCF/CASPT2 are taken into account for the spin-orbit interaction using the restricted active space state interaction (RASSI) method. We evaluated equilibrium bond distance (R_e), harmonic frequency (ω_e), rotational constant (B_e), dissociation energy (D_e and D_0), and transition energy (T_e) for the several low-lying states using the VIBROT program in MOLCAS. Starting from the near binding region (4.0 a.u.) to dissociation region (100 a.u.), we used a wide range of interatomic distances. Especially near the binding regions, 0.05 a.u. grid spacing is used to get accurate spectroscopic constants.

TDM and PDM calculations both at spin-free and spin-orbit levels based on the above potential energy curves are computed from the CASSCF wave functions. To check the accuracy of the PDM value at the equilibrium internuclear distance, we computed PDM at CASPT2 and CCSD(T) level of correlation invoking finite field perturbation theory (FFPT) with 0.0001 a.u. external field strength.

III. RESULTS AND DISCUSSION

A. Methodological study of ground state LiYb molecule

Table II shows bond length (R_e) and dissociation energy (D_e) values at various correlation levels with and without CPC. When we look at the data without CPC, the largest differences in R_e and D_e among all the basis sets are 0.28 Å and 1100 cm^{-1} at open-shell MP2, 0.18 Å, and 1300 cm^{-1} at CCSD(T), and 0.18 Å and 1300 cm^{-1} at CASPT2. In all the correlation methods, the R_e and D_e difference between basis 4 and 5 is much smaller than the corresponding difference between basis 1 and 2. At both CCSD(T) and CASPT2 level of correlation, the difference in D_e between basis 1 and 2 is about 700 cm^{-1} and it converges to 200 cm^{-1} for basis 4 and 5. At the same time, the convergence in R_e is much steeper with 0.11 Å between basis 1 and 2 and 0.02 Å between basis 4 and 5. These results indicate that the calculations using basis 5 are almost converged to the basis set limit. When we compare with and without CPC data in Table II, we can also understand how large the BSSE is in each method and basis set. BSSE is quite large in all the correlation calculations especially for smaller basis sets. For both CCSD(T) and CASPT2 calculations using basis 1, the D_e value without CPC is about twice larger than the one with CPC. However, using the biggest basis set (basis 5), the difference with and without CPC in D_e value becomes quite small; about 60 cm^{-1} at CCSD(T) and 110 cm^{-1} at CASPT2 level of calculations. Similar to D_e value, the difference in R_e value with and without CPC using the biggest basis is quite small (0.012 Å) in both CCSD(T) and CASPT2 methods. From these results, we consider using basis 5 is important for

TABLE II. Equilibrium bond distance R_e and dissociation energy D_e calculated in the supermolecule and the atomic limit of LiYb at open-shell MP2, CCSD(T), and CASPT2 levels of correlation. BSSE corrected R_e and D_e by the CPC are also listed.

Method	Basis	R_e (Å)	R_e(CPC) (Å)	Super molecular limit D_e (cm^{-1})	Atomic limit D_e (cm^{-1})	Super molecular limit D_e(CPC) (cm^{-1})	Atomic limit D_e(CPC) (cm^{-1})
Open-shell MP2	1	3.480	3.846	1909.90	1909.91	548.55	548.55
	2	3.636	3.812	1248.55	1248.55	598.56	598.55
	3	3.714	3.809	969.55	969.54	638.19	638.19
	4	3.701	3.785	952.34	952.34	699.39	699.38
	5	3.755	3.780	765.89	765.88	705.90	705.90
CCSD(T)	1	3.361	3.564	2808.30	2808.30	1278.34	1278.34
	2	3.472	3.564	2038.72	2038.72	1330.53	1330.53
	3	3.517	3.563	1741.41	1741.40	1390.58	1390.57
	4	3.518	3.553	1722.15	1722.16	1463.09	1463.09
	5	3.541	3.553	1531.72	1531.72	1473.79	1473.78
CASPT2	1	3.352	3.557	2748.97	2826.52	1303.60	1381.17
	2	3.461	3.558	2057.67	2127.29	1349.87	1419.53
	3	3.508	3.558	1701.26	1886.86	1286.03	1471.52
	4	3.511	3.511	1641.04	1852.45	1637.74	1849.05
	5	3.535	3.547	1377.28	1321.45	1277.41	1218.77

our further calculations of multielectronic states of LiYb. Also note that basis 5 is the largest RCC-ANO basis set distributed in MOLCAS.

The CASPT2 and CCSD(T) results show similar trend in bond length and dissociation energy, but the open-shell MP2 results show larger bond length and smaller dissociation energy than the CASPT2 and CCSD(T) ones. Also, the difference between CASPT2 and open-shell MP2 results indicates that taking an enough number of orbitals in CAS is essential and improves the description for electron correlation even for the ground state of LiYb. In principle, ground state of LiYb can be written with a single configuration in the whole region of the potential curve. This approximation is valid because LiYb dissociates to the ground state of Yb atom with a closed shell $(6s)^2$ and the ground state of Li atom with an open shell $(2s)^1$. Therefore, single reference correlation methods are qualitatively correct in this case and CCSD(T) is the most accurate and reliable method in the present calculations. CASPT2 provides similar values of CCSD(T) in our work: the deviations are only about 0.01 Å in R_e and 200 cm^{-1} in D_e. Noting the deviations to be acceptably small, we consider that CASPT2 also can provide accurate description for this system.

At the open-shell MP2, and CCSD(T) level, the value of D_e of the supermolecule Li–Yb with 100 a.u. internuclear distance is almost same as that of atomic limit Li+Yb because they are size-extensive methods. CASPT2 is known to provide almost size-consistent results.[25] Also in our CASPT2 calculations, the deviation between the atomic limit and supermolecule in the D_e value is about 50 cm^{-1} and reasonably small. Although, CCSD(T) is the most accurate method in this framework, it is not applicable for excited states of LiYb. Hence, instead of CCSD(T), we chose CASPT2 for the description of the multielectronic states for further calculations, as a reliable alternative of CCSD(T).

B. Potential energy curves and spectroscopic constants of the SF- and SO-CASPT2 calculations

Figures 1 and 2 represent the PECs of the LiYb ground and excited states at the spin-free and spin-orbit CASPT2 levels. In this calculation, we used basis 5 and neglected the BSSE effect since the corrections are negligible using basis 5, as shown in Sec. III A. For the spin-free level, we give term assignments for each PEC in Fig. 2 and here we explain the terms in Fig. 2 at the spin-orbit Ω level in detail. The molecular ground state (Ω=1/2) dissociates to the atomic ground states of Li($^2S_{1/2}$) and Yb($^1S_0$). The lowest three molecular excited states (two Ω=1/2 and one Ω=3/2) dissociate to the Li($^2P_{1/2,3/2}$)+Yb($^1S_0$) level, which corresponds to the first excitation of Li atom. Next five Ω=1/2, three Ω=3/2, and one Ω=5/2 states dissociate to Li($^2S_{1/2}$) +Yb($^3P_{0,1,2}$) and highest two Ω=1/2 and one Ω=3/2 states dissociate to Li($^2S_{1/2}$)+Yb($^1P_1$). Thus there are, in total, ten Ω=1/2, five Ω=3/2, and one Ω=5/2 states at the spin-orbit level, which dissociate to the excitations of Li 2*s*-2*p* and Yb 6*s*-6*p* orbitals. Examining the spin-free and spin-orbit potential energy curves, we find the structure to be similar except for the states dissociating to Yb(^3P) state, which shows more complicated levels due to spin-orbit effect.

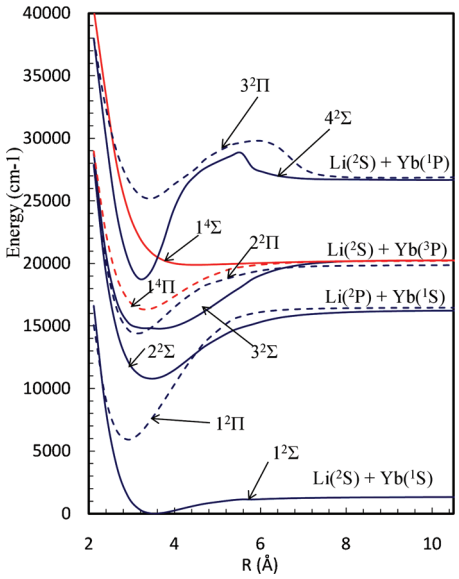

FIG. 1. Potential energy curves of low-lying states of LiYb molecule at the spin-free CASPT2 level. All the states are represented as following: (blue and red full lines) doublet and quartet Σ states and (blue and red dotted lines) doublet and quartet Π states.

The corresponding spin-free and spin-orbit spectroscopic constants are tabulated in Tables III and IV. Note that there is an experiment showing ground state spectroscopic constants of LiYb (R_e=2.920 Å, D_0=2792.02 cm^{-1}, and ω_e=354 cm^{-1}).[14] However, the present spin-orbit CASPT2 calculations provides somewhat different values such as R_e=3.529 Å, D_0=1421.96 cm^{-1}, and ω_e=135.54 cm^{-1}. The deviations between the experimental and theoretical values are to be analyzed more. Further experiments based on different techniques may be quite helpful for the discussion.

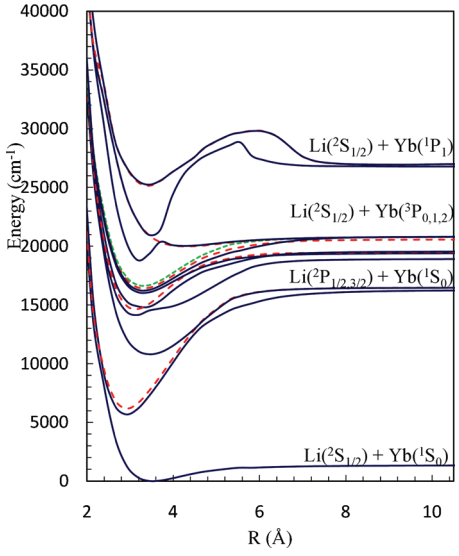

FIG. 2. Potential energy curves of low-lying states of LiYb molecule at the SO-CASPT2 level. Different Ω states are represented as following: (blue full lines) Ω=1/2; (red dashed lines) Ω=3/2; and (green dotted lines) Ω=5/2 states.

TABLE III. Equilibrium bond distance R_e, dissociation energy (D_e and D_0), adiabatic excitation energy T_e, harmonic frequency ω_e, and rotational constant B_e of the lowest nine energy levels by spin-free MS-CASPT2 calculation. A dense grid of 0.05 a.u. spacing around the equilibrium distance is used for fitting the potential curves. Supermolecular states with the bond length 100 a.u. are used to obtain dissociation energies.

MS-CASPT2 (Λ-S)	R_e (Å)	D_e (cm^{-1})	D_0 (cm^{-1})	ω_e (cm^{-1})	B_e (cm^{-1})	T_e (cm^{-1})
$1\ ^2\Sigma$	3.535	1477.61	1409.86	134.81	0.1975	⋯
$1\ ^2\Pi$	2.919	10 700.55	10 700.55	288.93	0.2924	5911.46
$2\ ^2\Sigma$	3.473	5480.53	5392.62	176.77	0.2068	10 782.63
$3\ ^2\Sigma$	3.641	5548.29	5499.89	97.67	0.1966	14 775.69
$2\ ^2\Pi$	3.127	5522.48	5401.49	241.50	0.2541	14 388.11
$1\ ^4\Pi$	3.318	3940.82	3844.04	193.83	0.2260	16 304.75
$1\ ^4\Sigma$	4.494	453.28	428.28	49.10	0.1198	19 890.69
$4\ ^2\Sigma$	3.239	7852.61	7657.42	389.81	0.2386	18 716.52
$3\ ^2\Pi$	3.418	1557.46	1440.51	233.28	0.2140	25 173.37

The spectroscopic parameters for the four lowest states both at the spin-orbit and spin-free level are comparable and are attributed to weak spin-orbit effect from Li ($^2P_{1/2,3/2}$) and Yb($^1S_0$) channels. In Fig. 1, the ground state shows a weaker bonding structure (larger R_e and smaller D_e) than the excited states dissociating to the first excited states of Li atom. This tendency can be explained from singly occupied molecular orbital (SOMO) nature in each state. By examining the CASSCF MO, we found that the SOMO of the ground state is a weak antibonding orbital, mainly consisting of Yb (6*s*) and Yb (2*s*) atomic orbitals. Contrary, the SOMO of the excited states corresponding to $1\ ^2\Pi$ and $2\ ^2\Sigma$ in spin-free notation are both nonbonding orbitals, consisting of only Yb (6*px*) and Li (2*pz*) atomic orbital, respectively. Since an antibonding orbital tends to expand compared to a nonbonding orbital, the trend of the SOMOs, we analyzed matches the potential energy curve characters.

All the other excited states higher than the four lowest states have more complex structure. One striking example of complicated potential curve is the fourth excited $\Omega=1/2$ state, which is showing a double minimum at the spin-orbit level. This effect is due to the strong coupling between the fourth and fifth 1/2 state arising from $3\ ^2\Sigma$ and $2\ ^2\Pi$ states. This effect is seen as a change in the R_e value with and without spin-orbit effects as $R_e=3.641$ Å (at the spin-free level), changing to $R_e=3.128$ Å and $R_e=3.386$ Å for the fourth and fifth 1/2 states. The second 3/2 state has similar spectroscopic constant as that of the $2\ ^2\Pi$ state as expected. The higher states (the sixth and seventh 1/2 state, third 3/2 state, and first 5/2 state) all arise from $1\ ^4\Pi$ spin-free state and hence have comparable spectroscopic constants. The fourth 3/2 state arising from $1\ ^4\Sigma$ spin-free state is also a shallow potential at spin-orbit level of calculation. All the other higher excited states leading to $Li(^2S_{1/2})+Yb(^1P_1)$ considered in the above calculation may not be accurate because we disregarded the excited states arising from excitations of 4*f*-5*d* and 6*s*-5*d* electrons which should lie below $^1P_1$ of Yb atom.

TABLE IV. Equilibrium bond distance R_e, dissociation energy (D_e and D_0), adiabatic excitation energy T_e, harmonic frequency ω_e, and rotational constant B_e of the low-lying energy levels by spin-orbit CASPT2-RASSI-SO calculation. A dense grid of 0.05 a.u. spacing around the equilibrium distance is used for the fit. Supermolecular states with the bond length 100 a.u. are used to obtain dissociation energies.

Spin-orbit term Ω	R_e (Å)	D_e (cm^{-1})	D_0 (cm^{-1})	ω_e (cm^{-1})	B_e (cm^{-1})	T_e (cm^{-1})
1/2	3.529	1489.71	1421.96	135.54	0.1982	⋯
1/2	2.919	10 602.96	10 457.78	290.32	0.2912	5672.24
3/2	2.925	10 461.01	10 317.44	287.53	0.2912	6171.54
1/2	3.467	5822.51	5733.79	178.38	0.2076	10 802.6
1/2	3.128	4828.03	4710.28	236.51	0.2536	14 136.15
1/2	3.386	4610.26	4535.25	150.10	0.2266	14 833.63
3/2	3.127	4907.08	4785.29	242.71	0.2544	14 639.84
1/2	3.310	3576.26	3483.51	186.26	0.2266	16 022.51
3/2	3.316	4210.21	4112.62	195.47	0.2263	16 410.97
5/2	3.313	4198.11	4099.71	197.08	0.2267	16 632.86
1/2	3.309	4646.56	4550.58	192.39	0.2268	16 215.43
3/2	4.304	870.27	831.56	77.18	0.1334	19 985.29
1/2	3.241	2122.04	1927.66	389.38	0.2383	18 752.30
1/2	3.597	6120.94	5777.35	687.72	0.1985	20 557.67
3/2	3.413	1694.57	1576.01	237.23	0.2146	25 151.20
1/2	3.425	1601.82	1488.09	227.26	0.2129	25 248.43

TABLE V. Low-lying atomic excitation energies of Li and Yb calculated from supermolecular LiYb states (R=100 a.u.) at the SO-CASPT2 level of calculation.

Ω	Theory (cm^{-1})	Expt.[a] (cm^{-1})	Difference (cm^{-1})	Error from expt. (%)	Dissociation channels
1/2	⋯	⋯	⋯	⋯	$Li(^2S_{1/2})+Yb(^1S_0)$
1/2	14 783.28	14 903.62	−120.34	0.8	$Li(^2P_{1/2})+Yb(^1S_0)$
1/2	15 130.04	14 903.96	226.08	1.5	$Li(^2P_{3/2})+Yb(^1S_0)$
3/2	15 141.09	14 903.96	237.13	1.6	
1/2	17 471.76	17 288.44	183.32	0.2	$Li(^2S_{1/2})+Yb(^3P_0)$
1/2	17 951.69	17 992.01	−40.32	0.3	$Li(^2S_{1/2})+Yb(^3P_1)$
3/2	18 007.24	17 992.01	62.24	0.6	
1/2	18 107.24	17 992.01	115.23	2.9	
3/2	19 128.35	19 710.39	−582.04	1.9	$Li(^2S_{1/2})+Yb(^3P_2)$
5/2	19 339.56	19 710.39	−370.83	1.8	
3/2	19 363.20	19 710.39	−347.19	1.8	
1/2	19 369.55	19 710.39	−340.84	1.7	
1/2	19 381.69	19 710.39	−328.70	1.7	
1/2	25 231.76	25 068.22	163.54	0.7	$Li(^2S_{1/2})+Yb(^1P_1)$
3/2	25 366.30	25 068.22	298.08	1.2	
1/2	25 370.59	25 068.22	302.37	1.2	

[a]Reference 18.

In Table V, excitation energies calculated at 100 a.u. bond distance are compared with the experimental atomic excitation energies as a check of the dissociation limits. Our asymptotic energy levels show a slight deviation from degeneracy; about 10 cm^{-1} for Li $^2P_{3/2}$, 50 cm^{-1} for Yb $^3P_1$, 250 cm^{-1} for Yb $^3P_2$, and 140 cm^{-1} for Yb $^1P_1$. These are artificial errors resulting from using lower symmetry (C_{2v}) instead of real symmetry ($C_{\infty v}$) of the system. Errors from the experimental data[18] are also listed in Table V and they are reasonably small as follows. All the energy levels obtained by excitations from Li atom (three levels) are found to be accurate to 1.3% (200 cm^{-1}). The $^3P_{0,1,2}$ excited levels from Yb atom have a range of accuracies among the nine excited states from 0.22% to 2.9% (150 to 260 cm^{-1}). The higher excited states with $^1P_1$ dissociation limits (three excited states) are accurate to around 1% (140 cm^{-1}).

C. Transition dipole moments from ground to excited states

Figure 3 presents TDMs from the ground state ($1\ ^2\Sigma$) to all the excited states as functions of nuclear distance at the spin-free level. All the transitions to $^4\Sigma$ and $^4\Pi$ states do not appear as they are spin forbidden. In molecular binding regions, transitions to all the excited $^2\Sigma$ and $^2\Pi$ states are nonzero, whereas in atomic regions, TDM matrix elements are nonzero only for the states dissociating to $Li(^2P)+Yb(^1S)$ and $Li(^2S)+Yb(^1P)$. This result is consistent with the atomic selection rules which forbid transitions from singlet to triplet states. Some of the TDM curves showed sudden jumps around 5.6 Å. This unsmooth structure in the TDM curve around R=5.6 Å is due to change in the main component of the singly occupied molecular orbital from Yb ($6s$) to Yb ($6pz$).

In Figs. 4(a)–4(c), the spin-orbit TDM functions from the ground ($\Omega=1/2$) to excited states dissociating to $Li(^2P)+Yb(^1S)$, $Li(^2S)+Yb(^3P)$, and $Li(^2S)+Yb(^1P)$ are represented, respectively. We also draw the corresponding spin-free TDM functions in gray color in Fig. 4 for reference. We only described the absolute values of Ω in each figure because we could not specify sign of Ω in the present analysis.

In Fig. 4(a), the second $\Omega=1/2$ and first $\Omega=3/2$ states correspond to the spin-orbit splitting of $1\ ^2\Pi$ state, and the third $\Omega=1/2$ state correspond to $2\ ^2\Sigma$ state. The similarity between the spin-free and spin-orbit curve is evident as expected from the analysis of the potential energy curves of these states. The spin-orbit TDM functions in Fig. 4(b) is more complicated than the functions in Fig. 4(a). This complication arise due to the existence of quartet states in this dissociation limit $[Li(^2S)+Yb(^3P)]$. This in turn leads to a large number of states with nonzero TDM value via spin-

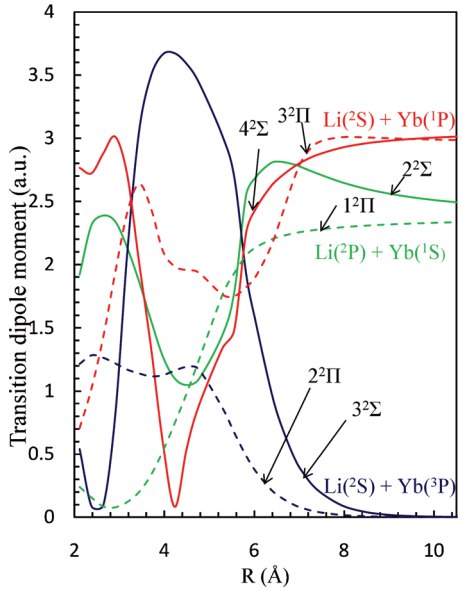

FIG. 3. Transition dipole moments from ground to excited states at spin-free CASSCF level of calculation. All the states are represented as following: (full lines) doublet Σ to Σ and (dashed lines) doublet Σ to Π states.

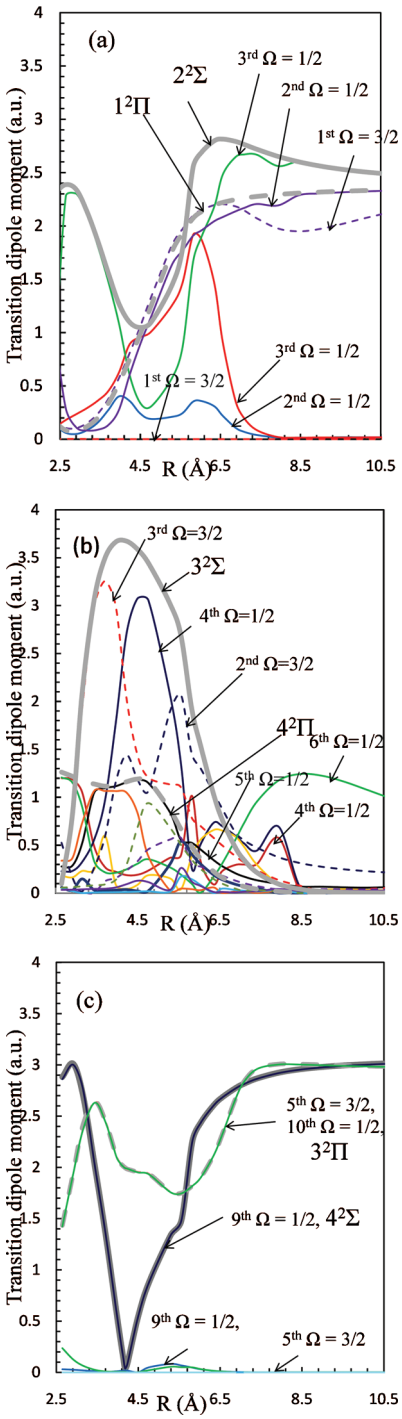

FIG. 4. Transition dipole moments from ground to excited states at spin-orbit CASSCF level of calculation considering only the states dissociating to (a) Yb(^{1}S)+Li(^{2}P), (b) Li(^{2}S)+Yb(^{3}P), and (c) Li(^{2}S)+Yb(^{1}P) limits. Different Ω states are represented as follows: (full lines) Ω=1/2; and (dashed lines) Ω=3/2 states. The spin-free TDM curves (wide gray lines) dissocating to the corresponding limit is also added to the respective graph for comparison.

orbit coupling. In Fig. 4(b), we have assigned Ω value only for major states with large value of TDMs, since the rest of states are too complicated to be analyzed. Although the TDM curves at the spin-free level (3 $^2\Sigma$ and 2 $^2\Pi$) asymptotically goes to zero at the atomic limit, we find TDMs to be nonzero at spin-orbit level for the second Ω=3/2, fifth, and sixth Ω=1/2 TDM curves. These nonzero TDM functions at large internuclear distance arise because of the spin-orbit interaction between the $^1P_1$ and $^3P_1$ atomic components. In Fig. 4(c), the spin-free and spin-orbit curves are almost identical. However, TDM functions in Fig. 4(c) may be less accurate as we have disregarded the intermediate states dissociating to Yb(^{3}D) limit in this work.

The accuracy of our TDM calculations are checked by comparing the results at dissociated regions (R=100 a.u.) with available experimental and theoretical atomic data of TDM. For Li atomic (2*s*-2*p*) transition, our calculated TDM value (2.362 a.u.) is quite close to the experimental counterpart (2.36 a.u.).[26] For Yb atomic $^3P_1((6s6p)$-$^1S_0(6s^2))$ transition, our calculated TDM value (0.146 a.u.) is reasonably comparable with the high accuracy atomic calculations (0.310 a.u.) (Ref. 27) and experimental results (0.315 a.u.).[28] For atomic Yb($^1P_1(6s6p)$-$^1S_0(6s^2)$) transition, our calculated TDM value (2.989 a.u.) corresponds to available experimental data (2.32 a.u.) (Ref. 29) and high accuracy calculations (2.54 a.u.).[27]

Finally, we briefly mention the calculated values of PDM of the ground state at equilibrium internuclear distance. The PDM value is important in finding the strength of the long range dipole-dipole forces. The computed PDM at the spin-free CASSCF level is 0.149 D (1D=3.336×10^{-30} cm) at the equilibrium internuclear distance (R_e=3.535 Å). With spin-orbit effect the PDM change is very small and it is around 0.152 D at R_e=3.529 Å. In comparison with other polar molecules such as KRb (Ref. 30) and RbCs,[31] PDM of LiYb is found to be very small. Expecting a change in PDM at higher correlation levels for a small value like this, we computed PDM for LiYb system using higher level of correlation methods such as CASPT2 and CCSD(T). The computed PDM at spin-free CASPT2 (−0.447 D at R_e=3.535 Å) and CCSD(T) (−0.110 D at R_e=3.541 Å) levels by invoking FFPT turns out to be negative values in comparison with spin-free CASSCF level of calculation. However, the absolute PDM values are still very small and are of same order at different correlation levels.

IV. CONCLUSIONS

To assist the ongoing photoassociation experiments on LiYb system, we have computed the ground and several low-lying excited states using *ab initio* quasirelativistic molecular orbital method. Starting from the spin-free third-order DKH Hamiltonian, we first examined the convergence of ground state dissociation energy and equilibrium bond length with five different contracted basis sets in RCC-ANO series. With these incremental basis sets for open-shell MP2, CCSD(T), and CASPT2, we found that the ground state dissociation energy converges with the increase in the basis set size. For the largest basis (basis 5), the CASPT2 and CCSD(T) methods provided results that are reasonably close to each other in the ground state. Hence, the potential energy curves including excited states were generated using basis 5, including spin-free and spin-orbit effects at the CASPT2 level. The spectroscopic constants of the ground and excited states are also proposed at the spin-free and spin-orbit level. The accuracy of the excited states calculation was confirmed by find-

ing the dissociation channels and comparing them with experimental atomic energies. All the calculated energy levels corresponding to Li or Yb atomic excitations are found to be accurate with less than 3% error. Permanent dipole moment of the ground state (~0.15 D) at the equilibrium internuclear distance is found to be small in magnitude. The small value of PDM in the ground state LiYb may not be advantageous for investigation of long range dipole-dipole forces. Apart from that, we analyzed transition dipole moment functions at both spin-free and spin-orbit levels. We obtained satisfying agreements of our calculated TDM values with available theoretical and experimental atomic results. The present TDM functions are important for further calculations of photoassociation intensities and spontaneous emission coefficients from/to the ground and excited electronic states considering rovibrational states. This work is underway and will be discussed in our future papers.

ACKNOWLEDGMENTS

We thank Professor Takahashi and Dr. Takasu of University of Kyoto and Professor Kanamori of Tokyo Institute of Technology for explaining the experimental details and the related theoretical details required for this work. We would also like to thank Professor Hossein Sadeghpour (ITAMP, Harvard Smithsonian Center for Astrophysics) for introducing this subject to us. One of the authors, M.A., thanks the Japan Society for the Promotion of Science.

[1] L.P. Pitaevskii and S Stringari, *Bose-Einstein Condensation* (Oxford University Press, New York, 2003).
[2] F. Dalfovo, S. Giorgini, L. P. Pitaevskii, and S. Stringari, Rev. Mod. Phys. **71**, 463 (1999).
[3] C. Pethick and H. Smith, *Bose-Einstein Condensation in Dilute Gases*, (Cambridge University Press, United Kingdom, 2002).
[4] B. DeMarco and D. S. Jin, Science **285**, 1703 (1999).
[5] C. Menotti, M. Lewenstein, T. Lahaye, and T. Pfau, AIP Conf. Proc. **970**, 332 (2008).
[6] J. Doyle, B. Friedrich, R. V. Krems, and F. Masnou-Seeuws, Eur. Phys. J. D **31**, 149 (2004), and references therein.
[7] W. Stwalley and H. Wang, J. Mol. Spectrosc. **195**, 194 (1999).
[8] P. Courteille, R. S. Freeland, D. J. Heinzen, F. A. van Abeelen, and B. J. Verhaar, Phys. Rev. Lett. **81**, 69 (1998).
[9] S. Inouye, K. B. Davis, M. R. Andrews, J. Stenger, H. J. Miesner, D. M. Stamper-Kurn, and W. Ketterle, Nature (London) **392**, 151 (1998).
[10] R. V. Krems, B. Friedrich, and W. C. Stwalley, *Cold Molecules: Theory, Experiment, Applications* (CRC, Boca Raton, 2009).
[11] M. Okano, H. Hara, M. Muramatsu, S. Uetake, Y. Takasu, and Y. Takahashi, The 21st Century COE Symposium, Kyoto University Clock Tower Centennial Hall, 2007, p. 48.
[12] A. Micheli, G. K. Brennen, and P. Zoller, Nat. Phys. **2**, 341 (2006).
[13] M. Okano, H. Hara, M. Muramatsu, K. Doi, S. Uetake, Y. Takasu, and Y. Takahashi, Appl. Phys. B: Lasers Opt. **98**, 691 (2010).
[14] A. Neubert and K. F. Zmbov, Chem. Phys. **76**, 469 (1983).
[15] G. Karlstrom, R. Lindh, P. A. Malmqvist, B. O. Roos, U. Ryde, V. Veryazov, P. O. Widmark, M. Cossi, B. Schimmelpfennig, P. Neogrady, and L. Seijo, Comput. Mater. Sci. **28**, 222 (2003).
[16] L. Gagliardi and B. O. Roos, Nature (London) **433**, 848 (2005).
[17] B. O. Roos, R. Lindh, P. A. Malmqvist, V. Veryazov, and P. O. Widmark, J. Phys. Chem. A **112**, 11431 (2008).
[18] J. E. Sansonetti, W. C. Martin, and S. L. Young, (2005), *Handbook of Basic Atomic Spectroscopic Data* (version 1.1.2). [Online] Available at http://physics.nist.gov/Handbook [2010, January 29]. National Institute of Standards and Technology, Gaithersburg, MD.
[19] N. Douglas and N. M. Kroll, Ann. Phys. **82**, 89 (1974).
[20] B. A. Hess, Phys. Rev. A **33**, 3742 (1986).
[21] Note that the ground state of LiYb is approximately a doublet system with an open-shell. Hence, HF energy of the system is equivalent to the CASSCF energy with one electron in highest occupied orbital in active space. Similarly, MP2 energy should be equivalent to the CASPT2 energy from the reference function of the above single-determinant CASSCF state. Because the SCF and MP2 energy for SCF and MBPT routine in MOLCAS are not effective for the open-shell doublet system, we used the above single-determinant CASSCF and CASPT2 energy for open-shell HF and MP2 energy.
[22] N. Forsberg and P.-Å. Malmqvist, Chem. Phys. Lett. **274**, 196 (1997).
[23] G. Ghigo, B. O. Roos, and P.-Å. Malmqvist, Chem. Phys. Lett. **396**, 142 (2004).
[24] B. A. Hess, C. M. Marian, U. Wahlgren, and O. Gropen, Chem. Phys. Lett. **251**, 365 (1996); B. Shimmelpfennig, Stockholm University (1996).
[25] J. M. Rintelman, I. Adamovic, S. Varganov, and M. S. Gordon, J. Chem. Phys. **122**, 044105 (2005).
[26] H. Partridge and R. S. Langhoff, J. Chem. Phys. **74**, 2361 (1981).
[27] S. G. Porsev, Yu. G. Rakhlina, and M. G. Kozlov, Phys. Rev. A **60**, 2781 (1999).
[28] C. J. Bowers, D. Budker, E. D. Commins, G. Gwinner, S. J. Freedman, J. E. Stalnaker, and D. DeMille, Lawrence Berkeley National Laboratory Report No. 42454, 1998.
[29] N. P. Penkin, K. B. Blagoev, and V. A. Komarovskii, *Atomic Physics VI* (Riga, Latvia, 1978).
[30] S. Kotochigova, P. S. Julienne, and E. Tiesinga, Phys. Rev. A **68**, 022501 (2003).
[31] S. Kotochigova and E. Tiesinga, J. Chem. Phys. **123**, 174304 (2005).